Between-session Reliability of Subject-Specific Musculoskeletal Models of the Spine Derived from Optoelectronic Motion Capture Data

[1,2]Katelyn Burkhart, [3]Daniel Grindle, [1,2]Mary L. Bouxsein, [1,2]Dennis Anderson

[1]Department of Orthopedic Surgery, Harvard Medical School, [2]Center for Advanced Orthopaedic Studies, Beth Israel Deaconess Medical Center, [3]Division of Engineering Mechanics, Virginia Polytechnic Institute and State University

Author Contact: kburkhar@bidmc.harvard.edu

Introduction

Marker placement on anatomical landmarks

Vicon motion capture

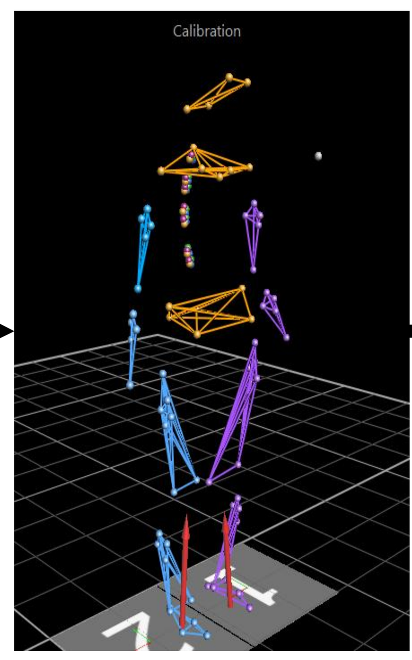

Musculoskeletal model scaling

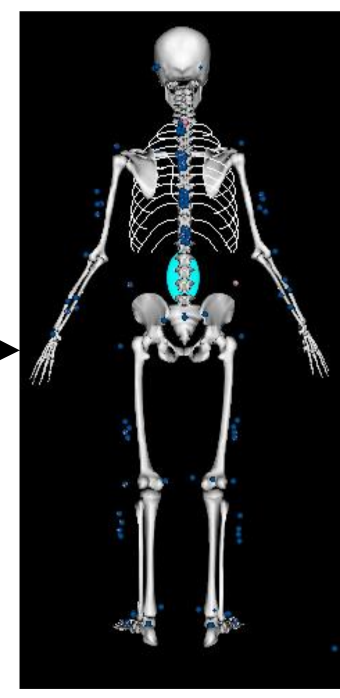

How does day-to-day variation in marker placement affect model outcomes?

Objectives

Investigate how between-session variation in placement of anatomical markers affects the reliability of subject-specific musculoskeletal models:

- **Body Segment Scaling**
- **Spine Curvature Estimation**
- **Compressive Spine Loading**

Study Design

Subject Data and Model Scaling

- 19 healthy participants (24-74 yrs), 2 sessions at least 1 day apart, 2 testers placed markers
- Retroreflective markers placed on: spine (C7, T1, T4, T5, T8, T9, T12 and L1 spine processes), pelvis, upper and lower limbs, and head

Model Creation, Scaling, and Spine Curvature

- Full body musculoskeletal models (Figure 1) scaled on marker measurements (Table 1)
- Used method from Nerot et al. to estimate intervertebral joint centers from marker data and set spine curvature in models

Spine Loading Estimations

- Each subject-specific model run through 5 standardized postures: standing, 45˚ trunk flexion, 15˚ trunk extension, 20˚ right lateral bend, and 45˚ right axial rotation.

Statistics

- Intraclass correlation coefficients (ICCs) and standard error of measurement were calculated as measures of between-session reliability and measurement error, respectively.

Body Segment	Axis	Scaled to distance between:
Head/Neck	S-I	C7 marker to head center
	M-L, A-P	Diagonal distance between headband markers
Humerus	All	Acromion marker to lateral epicondyle of the humerus
Radius/Ulna	All	Lateral epicondyle of humerus to radial styloid process
Spine (T1-L5 vertebral bodies)	S-I	C7 marker to mid-PSIS
	M-L, A-P	Height scale factor
Pelvis/Sacrum	M-L	ASIS-ASIS and PSIS-PSIS
	S-I, A-P	Mid - hip joint center and L5/S1 joint
Femur	All	Hip joint center to knee joint center
Tibia/Fibula	All	Knee joint center to ankle joint center
Foot (Talus, Calcaneus, Toes)	M-L, A-P	Heel marker to 1st MTP joint (big toe)
	S-I	Height scale factor
All other bodies	All	Height scale factor

S-I: Superior-inferior (height), M-L: Medio-lateral (width), A-P: Anterior-posterior (depth)

Table 1: Body segments scaling factor definitions

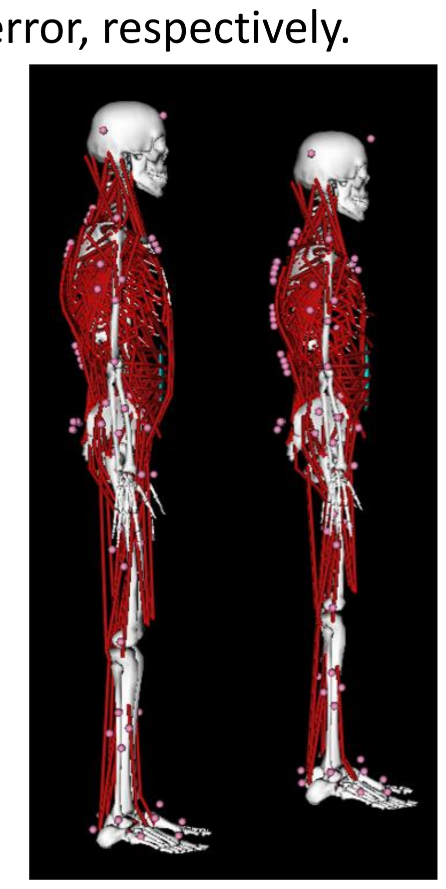

Figure 1: Male (left) and female musculoskeletal models

Acknowledgements

Rebecca Tromp and Javad Mousavi contributed to data collection. This work supported by grants from the National Institutes of Health (R00AG042458; R01AR073019), the Department of Orthopaedic Surgery at Beth Israel Deaconess Medical Center, and Harvard Catalyst (UL1 TR001102)

Results

Body Segment Scaling

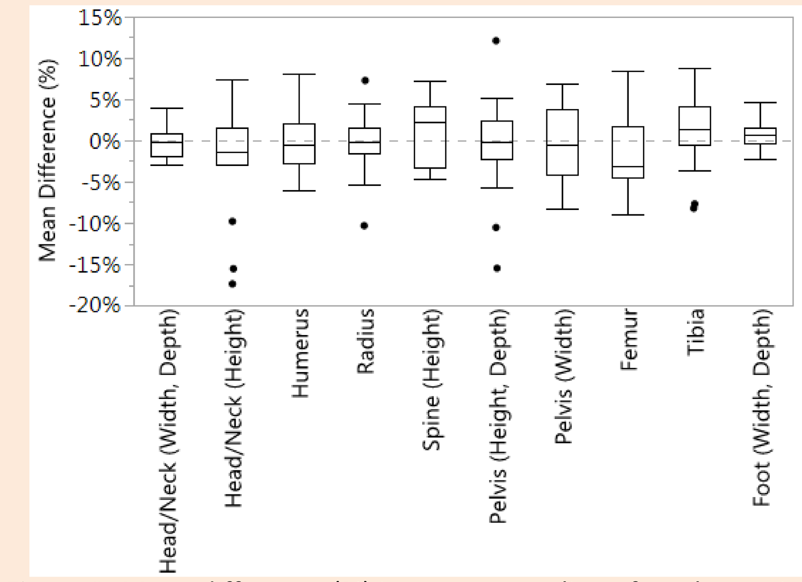

Figure 2: Mean difference (%) in segment scaling of marker-estimated anthropometry between sessions. Box plots show median and inter-quartile range, with black dots representing outliers.

Measurement	Mean (SD)	ICC (95% CI)	SEM
Head/Neck (Width, Depth)	20.9 (0.9)	**0.89** (0.71-0.96)	0.26
Head/Neck (Height)	18.2 (1.7)	0.75 (0.42-0.90)	0.90
Humerus	32.4 (1.8)	**0.81** (0.55-0.92)	0.81
Radius	25.3 (1.8)	**0.86** (0.66-0.95)	0.67
Spine (Height)	48.4 (3.7)	**0.85** (0.63-0.94)	1.44
Pelvis (Height, Depth)	10.3 (0.6)	0.46 (-0.005-0.76)	0.43
Pelvis (Width)	19.2 (1.1)	0.65 (0.28-0.86)	0.63
Femur	43.8 (2.0)	0.56 (0.14-0.81)	1.30
Tibia	39.3 (2.3)	0.68 (0.33-0.87)	1.30
Foot (Width, Depth)	20.6 (1.2)	**0.95** (0.87-0.98)	0.26

Table 2: Mean of Session 1 (SD), between-session ICCs (95% CI), and SEM of body segment scaling measures (in cm).

Spine Curvature

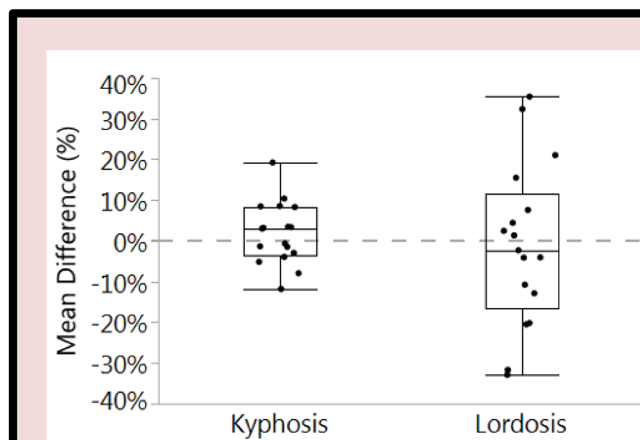

Figure 3: Mean (%) difference in marker-estimated spine curvature between sessions. Box plots show median and inter-quartile range, with black dots representing individual data points.

Measurement	Mean (SD)	ICC (95% CI)	SEM (degrees)
Kyphosis	40.3 (7.1)	**0.91** (0.77-.96)	2.2
Lordosis	50.5 (15.2)	**0.79** (0.52-.92)	7.0

Table 3: Mean of Session 1 (SD), between-session ICCs (95% CI), and SEM of marker-estimated spine curvature measures.

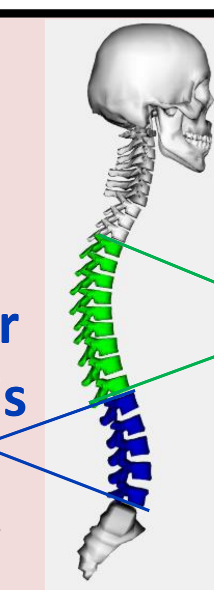

Compressive Spine Loading

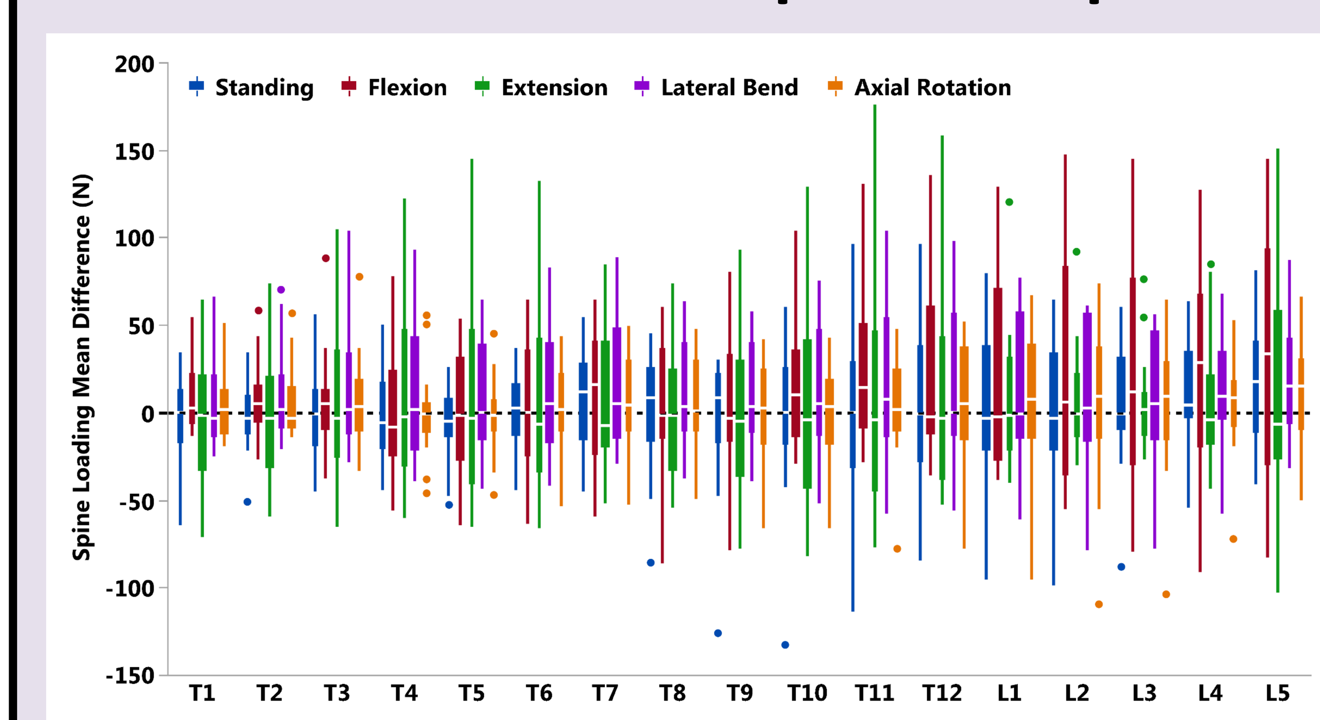

Figure 4: Mean difference in compressive spine load across spinal levels during 5 standardized activities. Box plots show median, interquartile range and range. Outliers are represented by dots.

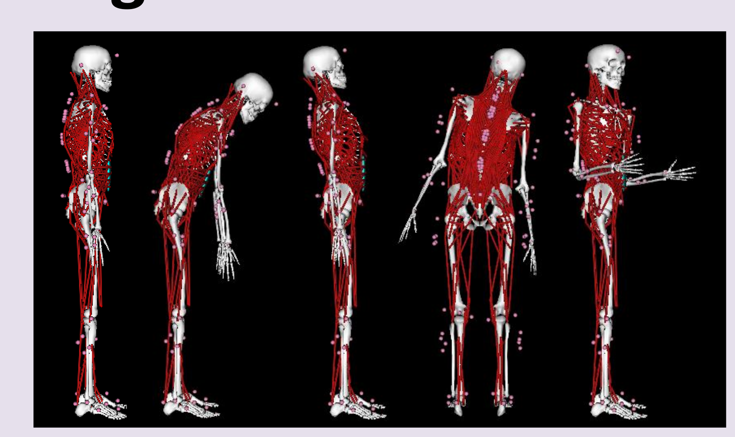

- Subject-specific spine loading between sessions was not significantly different for all activities.
- The ICC values of spine loading from T1 to L5 were mostly excellent, with 91% of ICC point estimates being greater than 0.75 for all activities.

Conclusions

- This is the first study to determine the reliability of spine loading determined from marker-based subject-specific musculoskeletal models.
- We found that larger differences in spine loading between sessions (>15%), at any level, were corresponding to larger differences (>10%) in lordosis or kyphosis between sessions.
- This indicates much of our spine loading differences can be ascribed, at least in part, to differences in spine curvature, and that precise and accurate assessment and implementation of spine curvature is crucial for creating subject-specific musculoskeletal models of the spine.

Overall, this information is a necessary precursor of using motion capture data to estimate spine loading with subject-specific musculoskeletal models, and suggests that marker data will deliver reproducible subject-specific models and estimates of spine loading. This informs the conduct and interpretation of future studies on dynamic spine loading, which are important for gaining insight into mechanisms contributing to back pain, vertebral fractures and other musculoskeletal injuries.